Research Inventy: International Journal of Engineering And Science
Vol.6, Issue 1 (January 2016), PP -17-24
Issn (e): 2278-4721, Issn (p):2319-6483, www.researchinventy.com

Simulation Modeling and Control of Hybrid Ac/Dc Microgrid

Dr.Ch Padmanabharaju[1], A Venkat Reddy[2]
[1,2] *EEE department, SreeDattha Institute of Engineering & Science*

Abstract: *This paper proposes simulation modeling and control of hybrid ac/dc micro grid. The micro grid concept introduces the reduction of multiple reverse conversions in an individual AC or DC grid and also facilitates connections to variable renewable AC and DC sources and loads to power systems. The interconnection of DGs to the utility/grid through power electronic converters has risen concerned about safe operation and protection of equipment's. The performance of proposed hybrid AC/DC micro grid system is analyzed in a grid-tied or autonomous mode. Here photovoltaic system, wind turbine generator and battery are used for the development of microgrid. Also control mechanisms are implemented for the converters for smooth power transfer and properly coordinate the AC sub-grid to DC sub-grid.*
The system is simulated in the MATLAB/ SIMULINK environment.
Index Terms: *Energy management, grid control, grid operation, hybrid micro grid, PV system, wind power generation.*

I. Introduction

The major challenges in electricity sector are: a) expanding access to electricity for sections of population not reached by the grid, and b) meeting increased demands from sections of populations within the reach of the grid. 20% penetration of RE in electricity generation globally is considered necessary in the coming decade (by 2020) [1]. Power systems are undergoing considerable change in operating Distributed generation based on wind, solar energy, biomass, mini-hydro along with use of fuel cells and micro turbines will plays attractive role both for grid fed and off grid systems. Advantages like environmental friendliness, expandability and flexibility have made distributed generation, powered by various renewable and nonconventional microsources, an attractive option for configuring modern Electrical grids.

II. Micro grid

Microgrid can be framed as an electrical system which includes electricity generation, energy storage, loads that normally operate along with the main utility grid and can disconnect and operate autonomously as well. The Microgrid consists of micro sources with power electronic interfaces. These micro sources usually are micro turbines, PV panels, and fuel cells, bio mass, bio gas are placed at customer sites. They are low cost, low voltage with reduced carbon emissions level. Power electronics interface provide the control and flexibility required by the Microgrid.

III. Hybrid Micro grid

Depending on locally available energy sources, Hybrid Micro grid systems can be developed often in combination with a storage element to match the available energy with the load. Many combinations are possible depending on local conditions, such as Wind-Diesel, Wind- Bio, Wind- Battery, Hydro-Bio, Wind-Solar, Hydro-Solar etc. Storage Systems includes Fuel Cells, Battery, Super Capacitor, Pump Storage, and Flywheel.

IV. Proposed Hybrid System

Fig.1 shows a hybrid microgrid system configuration where various ac and dc sources and loads are connected to the corresponding dc and ac networks. A renewable hybrid system, composed of PV panels and wind turbines as renewable energy sources, batteries as an electrical energy storage device, is considered. The AC and DC buses are coupled through a three phase transformer and a main bidirectional power flow converter to exchange power between DC and AC sides. The transformer helps to step up the AC voltage of the main converter to utility voltage level and to isolate AC and DC grids.

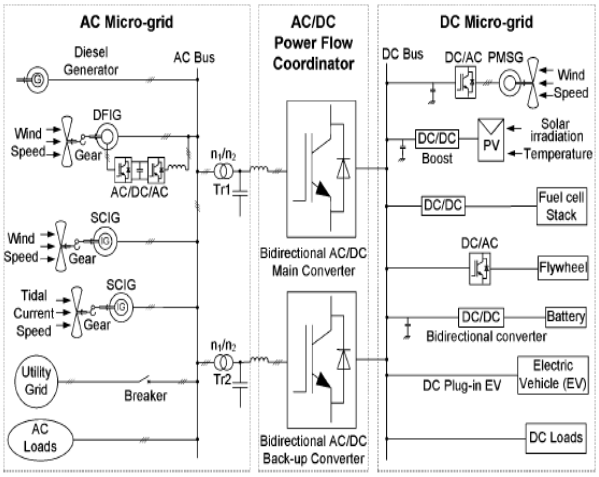

Fig.1 A hybrid ac/dc microgrid system.

V. Modelong of hybrid system

A schematic representation of hybrid grid is shown in Fig 2. It is modeled in the MATLAB/ Simulink to verify the operation of the system under various load and source conditions.

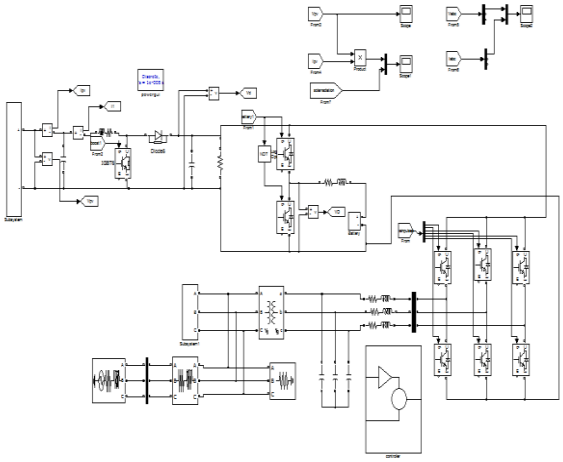

Fig.2 Proposed Hybrid System

VI. Mathematical Modeling And Simulink Of Wind-pv Hybrid Microgrid

A schematic representation of hybrid grid is shown in Fig 2. It is modeled in the MATLAB/ Simulink to verify the operation of the system under various load and source conditions. Doubly fed induction generator of 50kW rating is connected to ac bus as ac source. Forty kW PV arrays are connected to dc bus through a dc/dc boost converter as dc sources. A 65 Ah battery as energy storage is connected to dc bus through a bidirectional dc/dc converter. Variable dc load (20 kW–40 kW) and ac load (20 kW–40 kW) are connected to dc and ac buses respectively. The rated voltages for dc and ac buses are 400 V and 400 V rms respectively. A three phase bidirectional dc/ac main converter with R-L-C filter connects the dc bus to the ac bus through an isolation transformer. A wind generation system consists of doubly fed induction generator (DFIG) with back to back AC/DC/AC PWM converter connected between the rotor through slip rings and AC bus. A DFIG wind generation system is connected to AC bus to simulate AC sources. A variable DC and AC load are connected to their DC and AC buses to simulate various loads. The AC and DC buses are coupled through a three phase transformer and a main bidirectional power flow converter to exchange power between DC and AC sides. The transformer helps to step up the AC voltage of the main converter to utility voltage level and to isolate AC and DC grids. Boost converter, main converter, and bidirectional converter share a common DC bus. For grid tie PV system the output of the PV array is connected to DC-DC boost converter that is used to perform MPPT functions and increase the array terminal voltage. A DC link capacitor is used after the DC converter. An LC low pass filter is connected at the output of the inverter to attenuate high frequency harmonics and prevent them from propagating into the power system grid. The AC bus is connected to the utility grid through a transformer and circuit breaker. In the proposed system, PV arrays are connected to the DC bus through boost converter to simulate DC sources. Output of solar panel mainly varies due to solar radiation level and ambient temperature.

A battery with bidirectional DC/DC converter is connected to DC bus as energy storage. A capacitor Cpv is connected to the PV terminal in order to suppress high frequency ripples of the PV output voltage. In isolated mode the bidirectional DC/DC converter maintain the stable DC bus voltage through charging or discharging the battery. Modeling of the various components in the hybrid microgrid is described in the following section.

VII. Modeling of Wind Turbine

The aerodynamic model of the wind turbine gives a coupling between the wind speed and the mechanical torque produced by the wind turbine. Pm is the mechanical power produced by the wind turbine rotor can be defined as:

$$Pm = 0.5\,\rho A\,Cp(\lambda,\beta)\,V\omega^3$$

VIII. Modeling of PV Panel

The equivalent circuit of solar cell is given in Fig 3 .Current output of PV panel is modeled by the following equations [8],[11].

$$I_{pv} = n_p I_{ph} - n_p I_{sat}\left[\exp\left(\left(\frac{q}{AkT}\right)\left(\frac{Vpv}{ns} + IpvRs\right)\right) - 1\right]$$

$$Iph = (Isso + ki(T-Tr)).(S/1000)$$

$$Isat = Irr(T/Tr)3\exp((q\,Egap/kA).(1/Tr - 1/T))$$

Irr =Reverse saturation current

Iph = Photo current

Isat = model reverse saturation current

Ipv = Photovoltaic current

IX. Modeling of DFIG

d, q, s, and r denote d - axis, q - axis, stator and rotor Respectively. And) is the angular synchronous speed and slip speed respectively. L represents inductance And Flux linkage is. V and I represent voltage and Current respectively. Tm is mechanical torque Tem is the electromagnetic torque. The voltage equations of an induction machine in a rotating d - q coordinate are as

$$v_{ds} = Rsi_{ds} + \frac{d}{dt}\lambda_{ds} - (\omega_e\ \lambda_{qs})$$

$$v_{qs} = Rs\ i_{qs} + \frac{d}{dt}\lambda_{qs} + (\omega_e\ \lambda_{ds})$$

$$v_{dr} = Rr\ i_{dr} + \frac{d}{dt}\lambda_{dr} - (\omega_e\ \lambda_{qr})$$

$$v_{qr} = Rr\ i_{qr} + \frac{d}{dt}\lambda_{qr} + (\omega_e\ \lambda_{qr})$$

$$T_m - T_{em} = \frac{J}{n_p}\frac{d\ \omega_r}{dt}$$

X. Modeling and Control of Main Converter

To smoothly exchange power between dc and ac grids and supply a given reactive power to the ac link, control is implemented using current controlled voltage source for the main converter.[12] Fig. 4 shows the control diagram for the main converter. Two PI controllers are used to get real and reactive power control respectively. DC bus voltage is adjusted to constant through PI regulation whenever there is change in source conditions or load. When a sudden dc load drop causes power excess at dc side, the main converter is controlled to transmit power from the dc to the ac side. The active power absorbed by capacitor Cd leads to the rise of dc-link voltage. The negative error (Vd*-Vd) caused by the increase of Vd produces a higher active current reference id* through the PI control. The active current id and its reference id* are both positive. A higher positive reference will force active current id to increase through the inner current control loop. Therefore, the power excess of the dc grid can be transferred to the ac side. In the same way, a sudden increase of dc load causes the power lack and Vd fall at the dc grid. The main converter is controlled to supply power from the ac to the dc side. The positive voltage error caused by (Vd*-Vd) drop makes the magnitude of id* increase through the PI control. Because id and id* are both negative, the magnitude of id is increased through the inner current control loop. Therefore, power is transferred from the ac grid to the dc side.

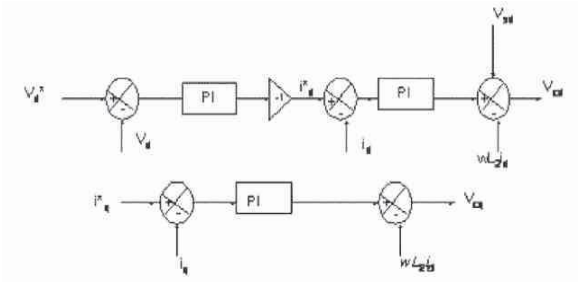

Fig.3 Control diagram of Main Converter

XI. Modeling & Control of Boost Converter

The boost DC-DC converter is used to step up the input voltage by storing energy in an inductor L1 for a certain time period, and then uses this energy to boost the input voltage to a higher value. The circuit diagram for a boost converter is shown in Fig When switch Q is closed, the input source charges up the inductor while diode D1 is reverse biased to provide isolation between the input and the output of the converter. When the switch is opened, energy stored in the inductor and the power supply is transferred to the load. The current and voltage equations at dc bus are as below

$$V_{pv} - V_T = L_1 \frac{di_1}{dt} + R_1 i_1$$

$$I_{pv} - i_1 = C_{PV} \frac{dV_{pv}}{dt}$$

$V_T = V_d(1 - d_1)$ $d_1$is the duty cycle ratio of switch Q.

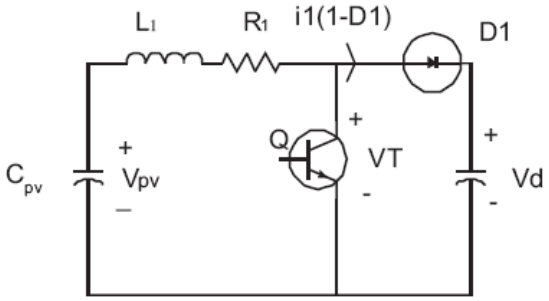

Fig. 4 Boost converter

The reference value of the solar panel terminal voltage is determined by the basic P&O algorithm to catch the maximum power. Dual loop control for the dc/dc boost converter has the objective to provide a high quality dc voltage. The outer voltage loop helps in tracking of reference voltage with zero steady state
error and inner current loop help to improve dynamic response.

Modeling and Control of Battery Converter

The battery converter is a bidirectional DC/DC converter and can be modeled as to provide a stable dc-link voltage. The dual loop control scheme is applied for the battery converter as shown in fig 6. The injection current is

$I_{in} = i_1 (1 - d_1) - i_{ac} - i_{dc}$. It should be noted that the output of the outer in 1 1 ac dc. Voltage loop is multiplied by -1 before it is set as the inner loop current reference.

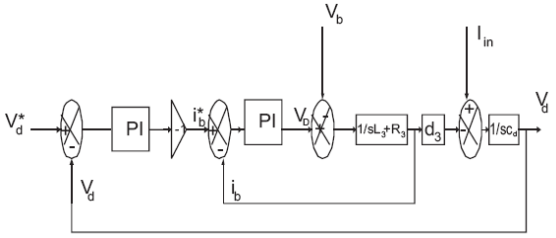

Fig 5 Control of battery converter

Current is defined positive when flowing into the battery, where the preset dc-link voltage is set to constant value. A decrease of Vdc caused by sudden load increase or decrease of solar irradiation, the positive voltage error (Vdc*-Vdc)multiplied by -1 through the PI produces a negative ib for the inner current loop, which makes the battery to transfer from charging into discharging mode and to rise Vdc back to its preset value . The battery converter is transferred from discharging into charging mode in the similar control method. The equations used for modeling of battery converter are

$$VD - Vb = L3. \frac{di_t}{dt} + R3\ ib$$

$$VD = Vd.\ d3$$

$$i1\ (1 - d1) - iac - idc - ibd3 = ic = Cd. \frac{dV_d}{dt}$$

XII. Simulation Results

Fig..6 shows the voltages of solar panel for various solar irradiations ranging from 400 w/m2 to 1000 w/m2 to 400w/m2 in grid connected mode. MPPT algorithm is tracking the optimal voltage from 0 to 0.2 sec.

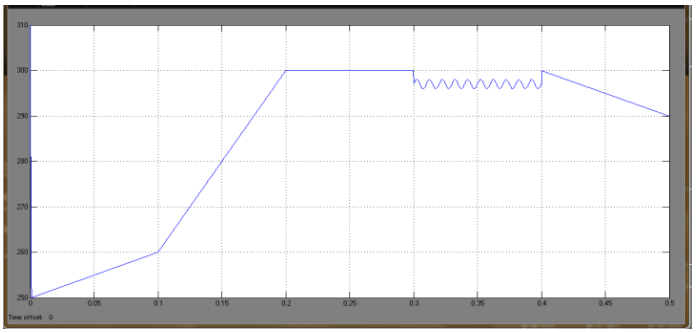

Fig. 6 Voltage of Solar Panel

Fig.7 shows the variation of power of solar panel with variable solar irradiation and constant load in grid connected mode. Power ranges from 13.5kW to 37.5kW with solar irradiation ranging from 400 w/m2 to 1000 w/m2 to 400 w/m2 . Solar irradiation changes at 0.1 sec from 400 w/m2 to 1000 w/m2. Power increases with the increase in solar irradiation where load is kept constant. At 0.3 sec solar irradiation decreased to 400 w/m2 so then power decreases after 0.3 sec.

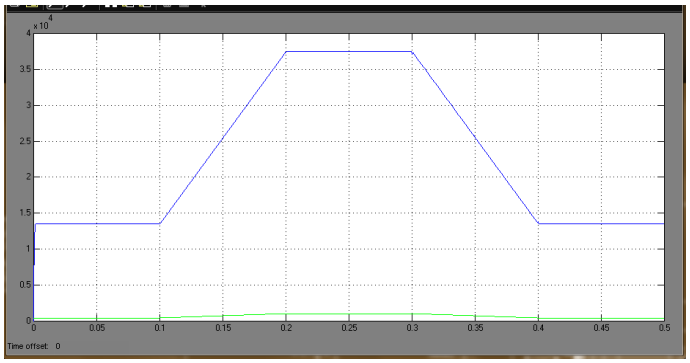

Fig. 7 Power Output of Solar Panel

Fig. 8 shows the voltage (voltage times 0.2 for comparison) and current responses at the ac side of the main converter when the solar irradiation level decreases from 1000W/m^2 at 0.3 s to 400W/m^2 at 0.4 s with a fixed dc load 20 kW. It can be seen from the current directions that the power is injected from the dc to the ac grid before 0.3 s and reversed after 0.4 s.

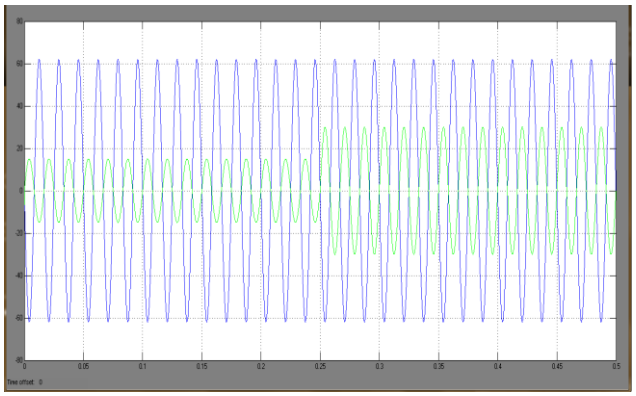

Fig.8 AC side voltage and current of the main converter with constant solar irradiation level and variable dc load

Fig.9 shows the voltage (voltage times 0.2 for comparison) and current responses at the ac side of the main converter when the dc load increases from 20 kW to 40 kW at 0.25 s with a fixed irradiation level 750W/m^2. It can be seen from the current direction that power is injected from dc to ac grid before 0.25 s and reversed after 0.25 s.

750 2

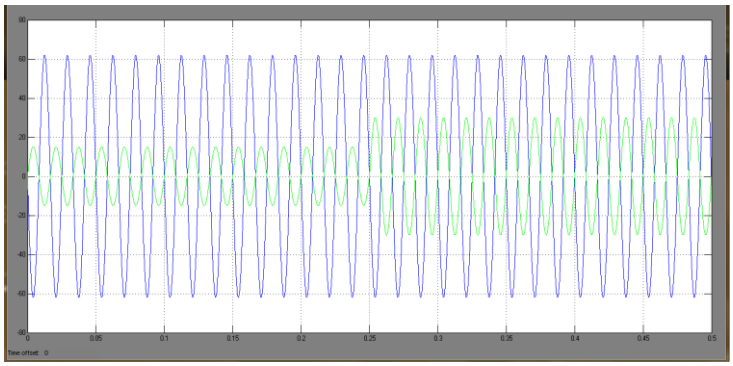

Fig.9 AC side voltage and current of the main converter with constant solar irradiation level and variable dc load.

Fig. 10 shows the voltage response at dc side of the main converter under the same conditions. The figure shows that the voltage drops at 0.25 s and recovers quickly by the controller.

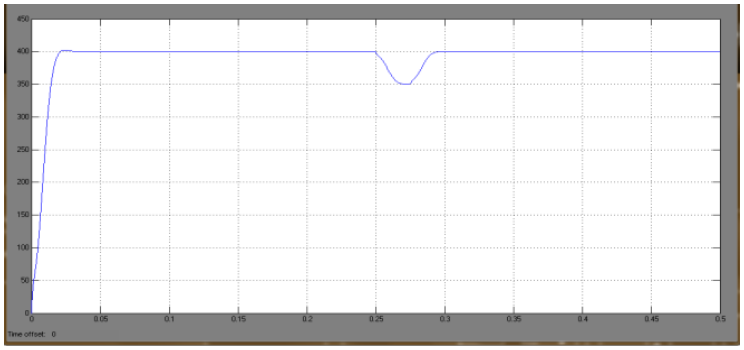

Fig.10 DC bus voltage transient response

XIII. Isolating Mode

Fig.11 shows the dynamic responses at the ac side of the main converter when the ac load increases from 20 kW to 40 kW at 0.3 s with a fixed wind speed 12 m/s. It is shown clearly that the ac grid injects power to the dc grid before 0.3 s and receives power from the dc grid after 0.3 s. The voltage at the ac bus is kept 326.5 V constant regardless of load conditions. The nominal voltage and rated capacity of the battery are selected as 200 V and 65 Ah respectively. Fig. 7.10 also shows the transient process of the DFIG power output, which becomes stable after 0.45 s due to the mechanical inertia.

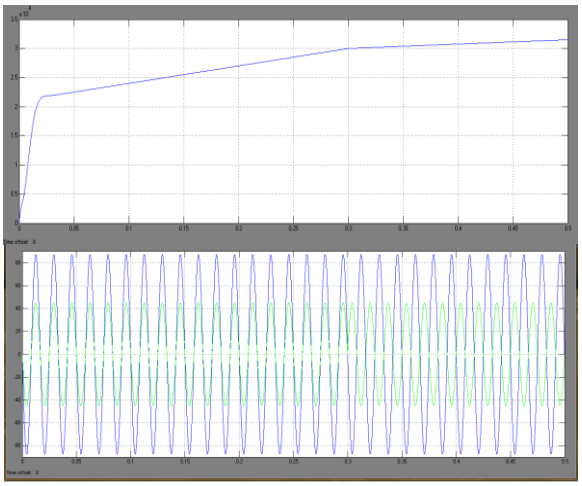

Fig. 11 Upper: output power of the DFIG; Lower: AC side voltage versus current (Voltage times 1/3 for comparison).

Fig.12 shows the current and SOC of the battery. Fig. 13 shows the voltage of the battery. The total power generated is greater than the total load before 0.3 s and less than the total load after 0.3 s. It can be seen from Fig. 12 that the battery operates in charging mode before 0.3 s because of the positive current and discharging mode after 0.3 s due to the negative current. The SOC increases and decreases before and after 0.3 s respectively.

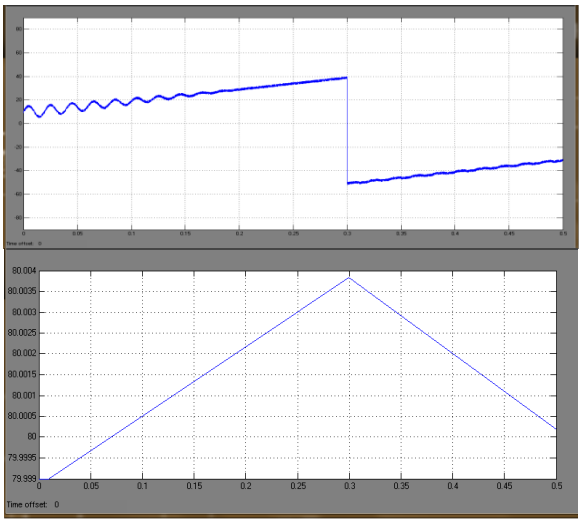

Fig. 12 Battery charging current (upper) and SOC (lower) for the normal case

When the system is at off-MPPT mode in Case 1, the dc bus voltage is maintained stable by the boost converter and ac bus voltage is provided by the main converter. Fig.14 shows the dc bus voltage, PV output power, and battery charging current respectively when the dc load decreases from 20 kW to 10 kW at 0.2 s with a constant solar irradiation level 1000 W/m^2.The battery discharging current is kept constant at 65 A. The dc bus voltage is stabilized to 400 V after 0.05 s from the load change. The PV power output drops from the maximum value after 0.2 s, which means that the operating modes are changed from MPPT to off-MPPT mode. The PV output power changes from 35 kW to 25 kW after 0.2 s.

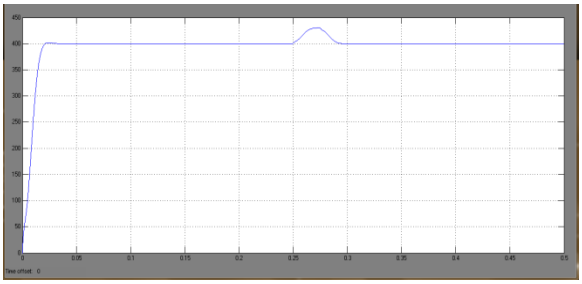

Fig. 14.1 DC bus voltage for Case 1

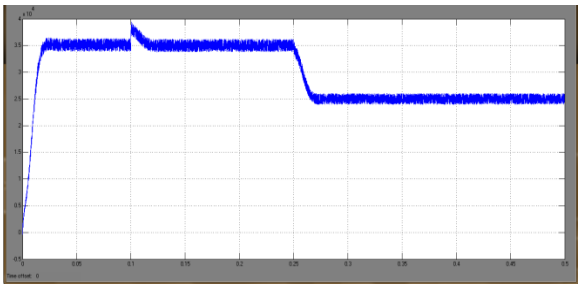

Fig.14.2. PV output power for Case 1

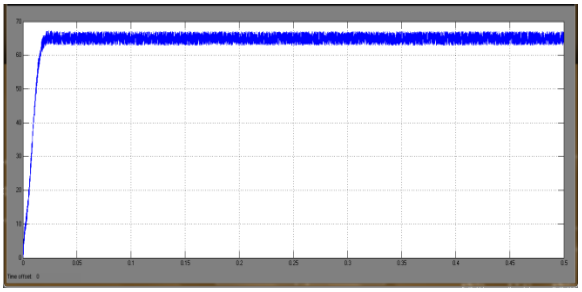

Fig. 14.3. Battery current for Case 1

XIV. Conclusion

A hybrid ac/dc microgrid is proposed and the modeling of hybrid microgrid for power system configuration is done in MATLAB/SIMULINK environment. The goal of this paper is to accelerate realization of the main benefit offered by smaller-scale Distributed Generation to use renewable energy. The coordinated control is proposed to Maintain stable system operation under various load and resource conditions. The microgrid concept enables high penetration of DG without requiring re-design or re-engineering of the distribution system itself. Although the hybrid grid can reduce the processes of DC/AC and AC/DC conversions in an individual AC or DC grid, there are lots of practical problems for the implementation of the hybrid grid based on the current AC dominated infrastructure. The hybrid grid may be feasible for small isolated industrial plants with both PV systems and wind turbine generator as the major power supply.

References

[1]. R. H. Lasseter, "MicroGrids," in *Proc. IEEE Power Eng. Soc. Winter Meet.*, Jan. 2002, vol. 1, pp. 305–308.

[2]. Y. Zoka, H. Sasaki, N. Yorino, K. Kawahara, and C. C. Liu, "An interaction problem of distributed generators installed in a MicroGrid," in *Proc. IEEE Elect. Utility Deregulation, Restructuring. Power Technol.*, Apr. 2004, vol. 2, pp. 795–799.

[3]. R. H. Lasseter and P. Paigi, "Microgrid: A conceptual solution," in *Proc. IEEE 35th PESC*, Jun. 2004, vol. 6, pp. 4285–4290.

[4]. C. K. Sao and P. W. Lehn, "Control and power management of converter fed MicroGrids," *IEEE Trans. Power Syst.*, vol. 23, no. 3, pp. 1088–1098, Aug. 2008.

[5]. T. Logenthiran, D. Srinivasan, and D.Wong, "Multi-agent coordination for DER in MicroGrid," in *Proc. IEEE Int. Conf. Sustainable Energy Technol.*, Nov. 2008, pp. 77–82.

[6]. M. E. Baran and N. R. Mahajan, "DC distribution for industrial systems: Opportunities and challenges," *IEEE Trans. Ind. Appl.*, vol. 39, no. 6, pp. 1596–1601, Nov. 2003.

[7]. Y. Ito, Z.Yang, and H. Akagi, "DC micro-grid based distribution power generation system," in *Proc. IEEE Int. Power Electron. Motion Control Conf.*, Aug. 2004, vol. 3, pp. 1740–1745.

[8]. A. Sannino, G. Postiglione, and M. H. J. Bollen, "Feasibility of a DC network for commercial facilities," *IEEE Trans. Ind. Appl.*, vol. 39, no. 5, pp. 1409–1507, Sep. 2003.

[9]. D. J. Hammerstrom, "AC versus DC distribution systems-did we get it right?," in *Proc. IEEE Power Eng. Soc. Gen. Meet.*, Jun. 2007, pp. 1–5.